Research Article

Journal of MASS SPECTROMETRY

Received: 4 December 2010 Accepted: 12 January 2011 Published online in Wiley Online Library: 2011

(wileyonlinelibrary.com) DOI 10.1002/jms.1894

Differentiation of human kidney stones induced by melamine and uric acid using surface desorption atmospheric pressure chemical ionization mass spectrometry

Bin Jia,[a] Yongzhong Ouyang,[a] Rana N. S. Sodhi,[b] Bin Hu,[a] Tingting Zhang,[c] Jianqiang Li[a] and Huanwen Chen[a]*

Clinically obtained human kidney stones of different pathogenesis were dissolved in acetic acid/methanol solutions and then rapidly analyzed by surface desorption atmospheric pressure chemical ionization mass spectrometry (SDAPCI-MS) without any desalination treatment. The mass spectral fingerprints of six groups of kidney stone samples were rapidly recorded in the mass range of *m/z* 50–400. A set of ten melamine-induced kidney stone samples and nine uric acid derived kidney stone samples were successfully differentiated from other groups by principal component analysis of SDAPCI-MS fingerprints upon positive-ion detection mode. In contrast, the mass spectra recorded using negative-ion detection mode did not give enough information to differentiate those stone samples. The results showed that in addition to the melamine, the chemical compounds enwrapped in the melamine-induced kidney stone samples differed from other kidney stone samples, providing useful hints for studying on the formation mechanisms of melamine-induced kidney stones. This study also provides useful information on establishing a MS-based platform for rapid analysis of the melamine-induced human kidney stones at molecular levels.

Keywords: surface desorption atmospheric pressure chemical ionization mass spectrometry; kidney stone; melamine; uric acid; principal component analysis

Introduction

The formation of kidney stones is related to both external and internal factors such as age, sex, family history of stone disease, occupation and working environment.[1] Variation in risk factors will often lead to the patients suffering from different types of kidney stones.[2] It has been reported that both humans[3] and animals[4] could be suffered from kidney stones due to ingestion of melamine illicitly used in the food. Although the causation of melamine-induced kidney stones can be retained for systematic studies, the unambiguous diagnosis of the melamine-induced human kidney stones is an urgent need for many purposes. For example, in China the government covers all the medical expenditures for the melamine-induced kidney stone diseases, but the patients suffering uric-acid-induced kidney stones have no 100% free medical care.[5] Therefore, accurate detection of melamine-induced human kidney stones is of great significance to both clinic diagnosis and economic interests.

Currently, infrared spectroscopy and Raman spectroscopy are the major methods for the clinic diagnosis of the urinary stones.[6,7] To date, these methods are useful for the identification of limited known categories of urinary stones. Also, these techniques do not lend themselves to quantitative analysis of the stone component in complex matrix[8] without sample cleanup. Generally, computed tomography (CT) is used as the gold standard for the diagnosis of urinary calculi, but there is no report indicated that CT could reliably differentiate the chemical composition (e.g. melamine) of the kidney stone samples.[9] The chemical elements in the stones such as calcium, phosphorus, oxygen, carbon and others can be detected by scanning electron microscopy with elemental distribution analysis (SEM-EDAX) combined with Fourier transform infrared spectroscopy (FTIR).[10] However, no report has demonstrated that this method determines melamine in the stone samples. Interim methods combined with ultrasonograph are widely used for the diagnosis of the urinary calculus caused by the melamine,[11–14] but the results are highly dependent on the clinical observations and statistics. So far there is no reliable method available for fast differentiating the melamine-induced kidney stone from other types.

Ambient mass spectrometry[15] represented typically by desorption electrospray ionization (DESI)[16–20] is of increasing interest for rapid detection of trace amounts of organic compounds present in complex matrices with minimal or no sample pretreatment. DESI and other similar techniques such as direct analysis

* *Correspondence to: Huanwen Chen, Jiangxi Key Laboratory for Mass Spectrometry and Instrumentation, East China Institute of Technology, Nanchang 330013, P. R. China. E-mail: chw8868@gmail.com*

a *Jiangxi Key Laboratory for Mass Spectrometry and Instrumentation, East China Institute of Technology, Nanchang 330013, P. R. China*

b *Surface Interface Ontario/Chemical Engineering & Applied Chemistry, University of Toronto, Toronto, Ontario, Canada M5S 3E5*

c *College of Information Science and Engineering, Harbin Institute of Technology at Weihai, Weihai 264209, P. R. China*

Table 1. Clinical data of human kidney stone samples

Patient code	Age	Sex	Quantity and period	Stone location	Imaging studies
Sample 1	26 months	Male	30–50 g/day, 2 years	Left ureter	Radiolucent
Sample 2	36 months	Female	30–50 g/day, 1.5 years	Left kidney pelvis	Radiolucent
Sample 3	7 years	Male	30–50 g/day, 2.5 years	Left kidney pelvis	Radiopaque
Sample 4	17 months	Male	30–50 g/day, 1.5 years	Left kidney pelvis	Radiopaque
Sample 5	48 years	Female	No drinking	Right ureter	Radiopaque
Sample 6	44 years	Male	No drinking	Left kidney pelvis	Radiopaque

in real-time (DART),[21–23] surface desorption atmospheric pressure chemical ionization (SDAPCI),[24–26] low-temperature plasma (LTP) probe,[27–29] electrospray-assisted laser desorption ionization (ELDI),[30–32] atmospheric pressure laser desorption/ionization (APLDI),[33] etc. are specially suitable for surface analysis, because the analyte ions are created on a 2-D surface of samples[16] under the ambient conditions, with no serious matrix interference.

Using ambient corona discharge for primary ion production, SDAPCI[24,25,34] successfully detects trace analytes on surfaces with improved sensitivity, due to the high density of the primary ions. A previous study has been made to analyze melamine tainted powdered milk samples using a home-made SDAPCI source, with minimal sample pretreatment.[35] The high sensitivity (LOD $= 3.4 \times 10^{-15}$ g/mm^2)[25] obtained showed that SDAPCI provided the potential feasibility for the detection of melamine in kidney stone samples. In this study, a new SDAPCI-MS-based method has been developed for direct analysis of kidney stone samples with minimal pretreatment. Melamine-induced kidney stone and uric-acid-derived kidney stone can be differentiated by performing principal component analysis (PCA) with the mass spectral raw data recorded using a positive-ion detection mode. Since neither time-consuming steps for separation of the sample nor expensive MS^n instrument for molecular structure identification is required to differentiate the melamine-induced kidney stone samples, the results indicated that the SDAPCI-MS-based method reported here should be a particularly useful tool for rapid differentiation of kidney stones at molecular levels.

Experiment

The human kidney stone samples were surgically removed from six patients and supplied by the Hospital of Gannan Medical University. As shown in Table 1, the patients from samples 1 to 4 were little children (no more than 7 years old) who had a history of drinking powdered milk (i.e. possible victims of melamine) during the periods of the melamine event[36] happened in China. It cannot be assured whether the powder milks consumed by these patients were contaminated with melamine, because the powder milk samples could not be collected at that time. However, as recorded in the clinical data sheet, patient 3, a 7-year old boy, really had consumed powdered milk for the longest time. Moreover, the preliminary work done by secondary ion mass spectrometry[37] in a Canada lab also showed that melamine was indeed found in the calculus from patient 3. The kidney stones of patients 5 and 6 who were adults had no milk products were used as the reference samples.

The kidney stone samples (1–5 mg) were dissolved in 10-ml acetic acid/methanol solution (1 : 4, v/v) and ultrasonicated for 20 min (10 W power) to assist the dissolution. The stone solution sample (20 µl) was placed on a sample holder (envelop paper), which was then carefully positioned in the SDAPCI source for ambient desorption/ionization.

Chemicals such as methanol (A.R. grade), acetic acid (A.R. grade) were bought from Chinese Chemical Reagent Co. Ltd. (Shanghai, China). All chemicals were directly used without any pretreatment other than dissolution and dilution with deionized water when necessary.

The experiments were carried out using a commercial linear ion-trap mass spectrometer (LTQ-XL, Finnigan, San Jose, CA) installed with a SDAPCI source. The SDAPCI source and the LTQ mass spectrometer were set to work in positive/negative-ion detection mode. The pressure of the sheath gas (N_2) was 0.05 MPa, the corona discharge voltage was $+3.5/-4.5$ kV and the temperature of the heated capillary was set to be 180 °C. Other parameters were default values of the instrument and no further optimization of the SDAPCI-MS was performed.

The full scan mass spectra were recorded with an average time of 30 scans, with subtraction of background. Collision-induced dissociation (CID) was performed with 20–37% collision energy (CE). The parent ions were isolated with a mass window width of 1.5 Da, and the MS/MS spectra were collected with a recording time of more than 30 scans if necessary.

PCA of the mass spectral fingerprint data was performed using the Matlab (version 7.0, Mathworks, Inc., Natick, MA, USA). The mass spectral data were exported to Microsoft Excel and the data were arranged using the *m/z* values as independent variables and using the relative abundance of the full-scan mass fingerprint (MS^1) as the dependent variables. The whole mass spectra data were treated as a matrix *X*, in which the rows and the columns corresponded to sample cases and *m/z* value variables, respectively. All the mass spectral data expressed by the relative abundance were directly used in the PCA processing. The 'princomp' function included in the 'Matlab Toolbox' was used for the PCA processing. When the PCA was completed, the scores and loadings of the first three principle components (PCs) were exported to new spreadsheets, and then Matlab was used to present the results of statistical analysis for better visualization.

Results and Discussion

SDAPCI-MS analysis

Positive-ion detection mode

As the first try, the original kidney stone samples were directly analyzed by SDAPCI-MS, without resorting to making the liquid solution samples. However, no useful signal for the original kidney stone could be recorded in these trials. Probably, this was due to the fact that the kidney stone samples were enwrapped by the

Journal of MASS SPECTROMETRY

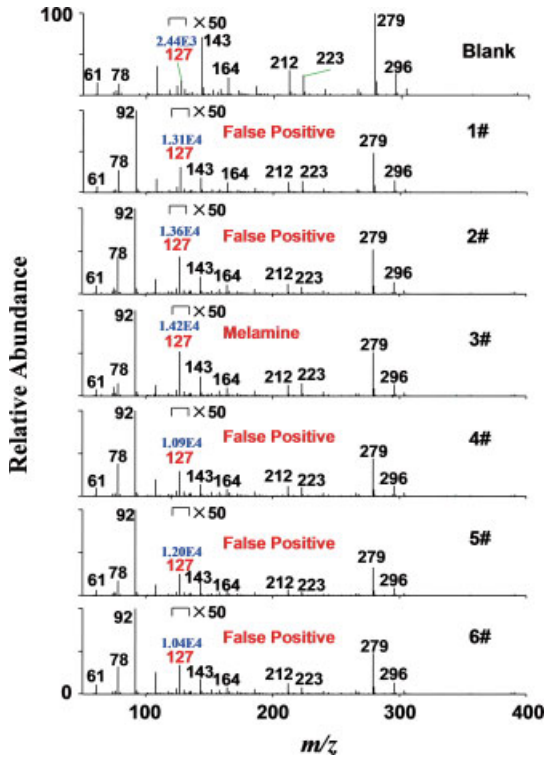

Figure 1. Positive SDAPCI mass spectra recorded from kidney stone solution samples. Blank: The empty paper surface used as a blank sample; 1#–6#: the stone obtained from patients 1–6, respectively.

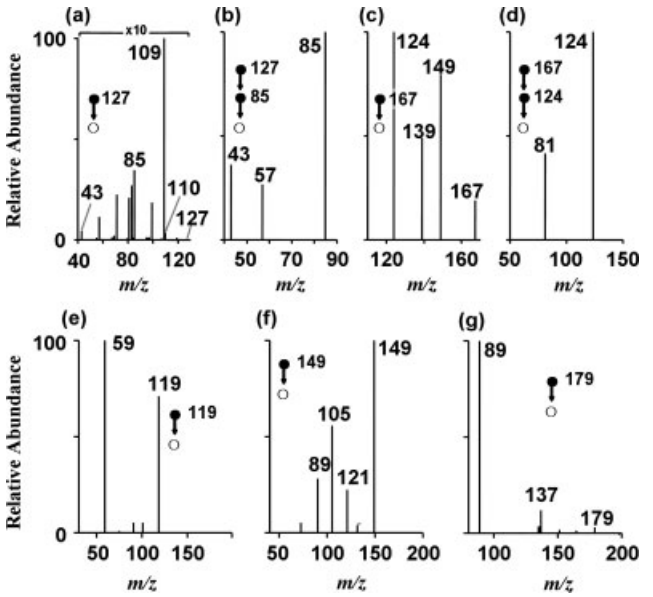

Figure 2. Mass spectra recorded by SDAPCI-MS. (a) MS/MS spectrum of protonated melamine (*m/z* 127) in sample 3; (b) MS/MS/MS spectrum of the ionic fragments (*m/z* 85) produced from protonated melamine (*m/z* 127) in sample 3; (c) MS/MS spectrum of deprotonated uric acid (*m/z* 167) in sample 2; (d) MS/MS/MS spectrum of the ionic fragments (*m/z* 124) produced from deprotonated uric acid (*m/z* 167) in sample 2; (e) MS/MS spectrum of deprotonated acetic acid dimer (*m/z* 119); (f) MS/MS spectrum of deprotonated cluster of acetic acid and oxalic acid (*m/z* 149) and (g) MS/MS spectrum of deprotonated oxalic acid dimer (*m/z* 179).

calcareous compounds, reducing the sensitivity of SDAPCI-MS for direct detection of organic compounds of the sample. Therefore, the solid stones were made into liquid solutions, which were then deposited on a paper surface for drying before the mass spectrometry analysis.

Using the positive-ion detection mode, the mass spectral fingerprints were recorded from the samples of the six patients, as shown in Fig. 1. For comparison, the mass spectrum of a blank sample (paper surface) was also obtained under the same experimental conditions. It is clear that, in the blank sample, the base peak (*m/z* 279) should be the protonated dibutyl phthalate (DBP)[38] used as a plasticizer in the instrument system. Although the signal of *m/z* 127 was recorded in the blank and all the six samples, the signal abundance of *m/z* 127 detected in the blank sample was in an order of magnitude less than those detected from the kidney stone samples. This result indicates that the peak at *m/z* 127 in the stone samples is likely to be the protonated melamine molecule $(M + H)^+$.[25] However, tandem MS data are required to validate the signals of *m/z* 127. In the CID experiments, only the precursor ions *m/z* 127 found in sample 3 generated three major fragments of *m/z* 43($C_2H_5N_4^+$), *m/z* 85 ($C_3H_4N_5^+$) and *m/z* 110 ($CH_3N_2^+$) by the loss of CH_2N_2, NH_3 and $C_2H_4N_4$, respectively (as shown in Fig. 2(a)), and moreover, the fragment *m/z* 85 successively produced fragment *m/z* 43 ($CH_3N_2^+$) in MS^3 experiment (Fig. 2(b)). Those fragmentation patterns were in agreement with the previous observations, which were the characteristic fragments[25,34,39] of melamine. The characteristic fragments observed in the tandem MS experiments confirmed that the peak at *m/z* 127 detected from sample 3 was correctly assigned to the protonated melamine. On the contrary, the precursor ions (*m/z* 127) of the other samples (except for sample 3) did not produce these characteristic fragments during the CID experiments, indicating that the mass spectrometric results of samples 1, 2, 4, 5 and 6 were not derived from melamine. In comparison with the mass spectra obtained from the blank and the kidney stone samples, a few peaks with abundant signal intensities (such as *m/z* 61, 78, 143, 164, 212, 223 and 296) appeared in both of the spectra, but some peaks such as *m/z* 92 and 106 were detected with significantly lower abundances from the blank than the samples. Besides the highly abundant peaks dominated in the mass spectra, there are many 'grassy' peaks showed up in the mass spectra recorded from the kidney stone samples. Since the kidney stone samples were formed inside the human kidney with quite a few months, it is reasonable to expect that the chemical profile of the melamine-induced kidney stone samples differs, in a degree, from that of the other types of kidney stone samples. If the difference between the chemical profiles of the kidney stone samples can be clearly detected using a method combined with SDAPCI-MS and PCA, the fast screening of the melamine-induced kidney stone samples might be completed without performing any sophisticated tandem MS measurement, thus greatly reducing the requirement of expensive instrument. This was further discussed with more data in the Principal Component Analysis Section.

Negative-ion detection mode

The alkaline melamine molecule was more likely to get protons, so normally it could not be detected upon the negative-ion detection mode. However, the negative SDAPCI-MS can be used as an ancillary tool for the diagnosis of other types of kidney stones. This is because that, in some cases, melamine stone was radiolucent as the uric acid stone,[40] and hence the melamine stones may be falsely diagnosed as uric acid stones upon X-ray examination.

Fortunately, uric acid molecule was easily deprotonated upon the negative-ion detection mode, so the SDAPCI-MS could be used as ancillary means in X-ray imaging study to exclude the interference from the uric acid in stone samples in identifying the melamine stone. Examination of these samples by time-of-flight secondary ion mass spectrometry (ToF-SIMS) at the University of Toronto[37] showed that the content of N-containing species increased greatly in samples 2 and 3, but the origins of the N-containing species (i.e. the N-containing species may come from either the melamine molecule or the uric acid molecule) could not be ascertained. Thus, further studies are required using techniques such as SDAPCI rather than SIMS to obtain the information at the molecular level.

The stone solution samples were also analyzed by SDAPCI-MS upon negative-ion detection mode. As the results, the mass spectral fingerprints of the six patients' stone samples and the blank sample (paper surface) were shown in Fig. 3. In the mass spectra of the blank sample, the major peaks were detected at *m/z* 89 and 179, which corresponded to deprotonated oxalic acid molecule and its dimer ($(2M - H)^-$), respectively. These high-level signals were probably ascribed to the relatively high gas-phase acidities. Upon CID, the precursor ions of *m/z* 179 mainly generated ions of *m/z* 89 (Fig. 2(g)), showing characteristic neutral loss of the deprotonated oxalic acid dimers. The abundance of peaks at *m/z* 59, 119 and 149 was increasingly detected when the stone solution samples were analyzed by SDAPCI-MS. Upon CID, the precursor ions of *m/z* 119 (deprotonated dimer of acetic acid) generated ions of *m/z* 59 (deprotonated acetic acid) by the loss of CH_3COOH (Fig. 2(e)); the precursor ions of *m/z* 149 (deprotonated cluster of acetic acid and oxalic acid) produced three major fragments of *m/z* 89, 105 and 121 by the loss of CH_3COOH, CO_2 and CO, respectively (Fig. 2(f)). The peak at *m/z* 167 was recorded with enhanced signal levels for all six samples rather than for the blank sample. Upon CID, the precursor ions of *m/z* 167 generated the abundant fragments of *m/z* 124 ($C_4H_2N_3O_2^-$) by the loss of CHNO (Fig. 2(c)), and the fragments of *m/z* 124 successively produced the major fragments $C_3HN_2O^-$ (*m/z* 81) in MS^3 experiment (Fig. 2(d)) by the loss of 43 units (CHNO). These characteristic fragments were in good agreement with those published data of uric acid.[41] Furthermore, the CID data also matched that using authentic uric acid compound under the same experimental conditions. Therefore, the ions of *m/z* 167 in the samples were assigned to be deprotonated uric acid. Interestingly, in comparison with other samples, the signal abundance of *m/z* 167 for sample 2 was significantly higher than other cases, indicating that the content of uric acid in the stone sample of patient 2 should be much higher than the others.

In a related study,[37] the same groups of samples were investigated using ToF-SIMS. Polished cross-sections of the samples were obtained for recording SIMS mass spectra in both high spatial and high mass resolution modes.[42] The motivation was to distinguish different stone types using the distribution patterns of the N-containing species obtained in the ToF-SIMS experimental data. Although some interesting data were obtained,[37] the SIMS technique was not able to separate the melamine-induced stone sample from other types such as the uric-acid-derived kidney stone samples. The results obtained using SDAPCI-MS in this work differentiate melamine-induced kidney stones from the uric-acid-based kidney stones, showing that SDAPCI-MS provides complementary information for the ToF-SIMS results. The combination of these two techniques is particularly useful for understanding the formation mechanism of the kidney stones. For clinical diagnosis purpose, however, SDAPCI-MS is of obvious advantages including simple operation,

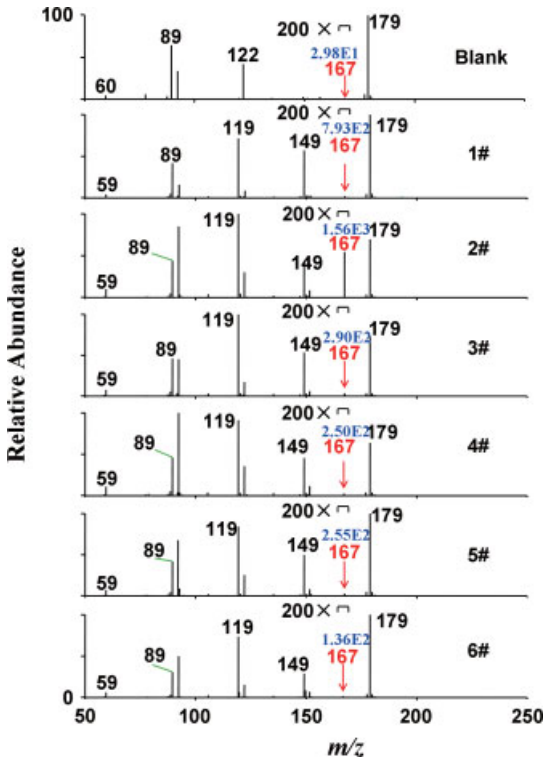

Figure 3. Negative SDAPCI mass spectra recorded from kidney stone solution samples. Blank: The empty paper surface used as a blank sample; 1#–6#: the stone obtained from patients 1–6, respectively.

low cost instrument and fast analysis speed, etc., especially when PCA is applied to process the experimental data (demonstrated in the next section).

Principal component analysis (PCA)

As mentioned above, the melamine and uric-acid-induced human kidney stones can be identified using the positive and/or negative mode of SDAPCI-MS/MS experiments. However, the sensitive CID measurements require an instrument of advanced tandem MS capability. This requirement demands expensive mass spectrometers, which are difficult to be miniaturized for *in situ* applications. As shown in the full-scan mass spectra, more signals rather than the melamine itself (*m/z* 127) were differentiable in the mass spectral fingerprints. Once the differences are clearly visualized with high confidence, the melamine-induced kidney stones can be reliably diagnosed without resorting to tandem MS experiments, featuring on site applications even using simple, low-cost portable mass spectrometers. Therefore, PCA, a powerful tool for data compression and information extraction,[43,44] was employed to process the SDAPCI-MS data for differentiation of the samples. As the result, a PCA score plot of six types of stone samples was shown in Fig. 4, among which a1 and a2 corresponded to the data of SDAPCI mass spectrum recorded upon positive-ion detection mode. Note that nine pieces of the stone samples from the same patient were analyzed for the groups of patients 1, 2 and 6, generating nine data points for patients 1, 2 and 6; but ten pieces of the stone samples from the same patient were analyzed for the groups of patients 3, 4 and 5; hence, there are ten data points for patients 3, 4 and 5. As shown in Fig. 4, a total of 57 data points was explained by the score graphs of PC1–PC2 and PC2–PC3. 95.6%

Journal of MASS SPECTROMETRY

of the total variations were represented and the percentages of variance explained by PC1, PC2 and PC3 were 80.02%, 12.28% and 3.30%, respectively. These PCs showed a good distinguishing ability, because both the melamine and uric-acid-induced stones were stayed in remarkably different areas of the PC space. In the PC1–PC2 graph (Fig. 4(a1)), the points of sample 3 (melamine-induced stones) was differentiated from other samples on the main direction of PC2. Samples 1 and 5 showed some resemblance in PC2, but they were separated on the direction of PC1. Samples 2, 4 and 6 were mixed together in the PC1–PC2 graph, but the direction of PC3 showed some useful information, as shown in the PC2–PC3 graph (Fig. 4(a2)), which left sample 2 (uric-acid-derived stone) isolated. According to these plots, except for samples 4 and 6 which cannot be distinguished from each other, the others were all differentiated from each other. As shown in the clinical data (Table 1), sample 1 showed different X-ray imaging properties from sample 5. This could be the major facts which could be accounted for the separation of samples 1 and 5 in the PCA score plots. The stones in patients 4 and 6 were both located in the left kidney pelvis and were all radiopaque in the X-ray imaging studies performed in the clinical examination. Accordingly, these two samples were not be distinguished from each other in the PCA score plots. Although the stone in sample 5 was also radiopaque, the location of the stone 5 was at the right ureter instead of the left kidney pelvis. This might be the main factors differentiating sample 5 from either sample 4 or 6. Similar to sample 5, sample 1 stones were also located in the ureter (the left one), but it was radiolucent in the X-ray imaging study, indicating that the chemical composition of sample 1 should be different from the others. This probably was attributed to the separation of sample 1 from the rest samples. In the PCA score plots, sample 2 is located remarkably far from sample 3, because sample 2 was uric-acid-induced kidney stones, which should be quite different from the melamine-induced kidney stones in terms of chemical composition. In summary, it is a useful notion that the formation mechanisms (with/without melamine), location and imaging property of kidney stones play important roles for differentiation of the types of kidney stones by performing PCA.

PCA was also employed to process the mass spectral data set in which the highly abundant peaks such as *m/z* 143, 164, 186, 212, 223 and 279 had been deleted. A total of 57 data points was explained by the score graphs of PC1–PC2 (Fig. 4(c1)) and PC2–PC3 (Fig. 4(c2)). 95.1% of the total variations were represented and the percentages of variance explained by PC1, PC2 and PC3 were 70.06, 16.45 and 8.56%, respectively. The score plots showed that the similarities and differences between the samples were in good agreement with the PCA results obtained using the full-scan spectral data set, although the separation pattern might not exactly the same. Therefore, these results demonstrated that the peaks detected by SDAPCI-MS with low abundances also have significance for differentiation of the kidney samples.

The PCA loadings obtained based on the positive-ion detection mode are also shown in Fig. 5. The predominant ions have been highlighted in the loading plots, such as protonated molecules at *m/z* 61, 65, 75, 78, 93, 108, 143, 164, 186, 212, 223 and 279. The most predominant ions in the loading of PC1 were the protonated DBP molecules (*m/z* 279), which was a negative contribution and served as the most important factor differentiating patient 5 from the others. With a relative greater score value in the positive direction of PC1 indicates that the relative abundance of *m/z* 279 in sample 5 should be lower than that in other samples. This is also consistent with the mass spectral fingerprints of these samples (Fig. 1). The abundance of the base peak (*m/z* 92) in sample 5 was about 25% higher than that in other samples. Therefore, the ions of *m/z* 92 may be the potential biomarkers for discriminating kidney stone types. In comparison with PC1, the PC2 did a better performances to differentiate kidney stones induced by melamine (patient 3) from other samples, with a relatively greater score value in the negative direction of PC2. Also, the peak at *m/z* 78 was predominant in PC2, indicating that the relative abundance of the peak at *m/z* 78 in the MS spectrum recorded from the melamine-induced stones (sample 3) should be lower than that in other samples. Similarly, indicating by the loading of PC3, the relative abundance of *m/z* 75 in the uric-acid-derived stones (patient 2) should be evidently higher than that in other samples. Therefore, the ions of *m/z* 78 and 75 may be the potential biomarkers for the differentiation of melamine-induced and uric-acid-derived kidney stone. With the information of these ions highlighted in the loading plots, other constituent peaks such as *m/z* 92, 78 and 75 might be used as biomarkers for discriminating kidney stone types. These results demonstrated that the useful information about stone samples had been recorded by PCA of the mass spectral fingerprints, although the peak intensities were relatively low.

The fingerprints data recorded under negative-ion detection mode were also used in the PCA, as shown in Fig. 4(b1 and b2). However, the score plots showed that the peaks collected by negative SDAPCI-MS did not provide enough information for successful differentiation of the different stone samples. This could be because that the peaks recorded by the negative SDAPCI-MS from different samples were too similar to be used for differentiation of the samples. In some cases, the formation of kidney stone was accompanied with the increase in pH value of urine.[45] In such case, the compounds with high gas-phase basicities are likely to be enwrapped inside the kidney stones since the pH value of the urine sample is increased; however, the basic compounds are unlikely to be detected as they are tended to be sensitively protonated for the detection under the positive-ion detection mode. Therefore, negative SDAPCI-MS is not proposed for the differentiation of the kidney stone samples without CID experiments.

Conclusions

A SDACPI-MS-based method was developed as a novel tool for the separation of melamine-induced and uric-acid-derived human kidney stone samples with minimal sample pretreatment. The results showed that the information recorded from positive SDACPI-MS mass spectral fingerprints were effective for reliable separation of the melamine-induced kidney stone samples. Without the need of tandem MS capability, the SDAPCI-MS combined with PCA is a powerful analytical tool for the differentiation of human kidney stones of different types, especially useful in the analysis and detection of melamine-induced kidney stones. However, the negative SDAPCI did not provide enough information for the differentiation of different stone samples, probably because the detected signals were too similar to differentiate each sample under the negative-ion detection mode. The experimental data demonstrate that besides the melamine itself many other chemicals detected from the melamine-induced kidney stone samples are different from those detected from kidney stone samples involving no melamine. This serves as the

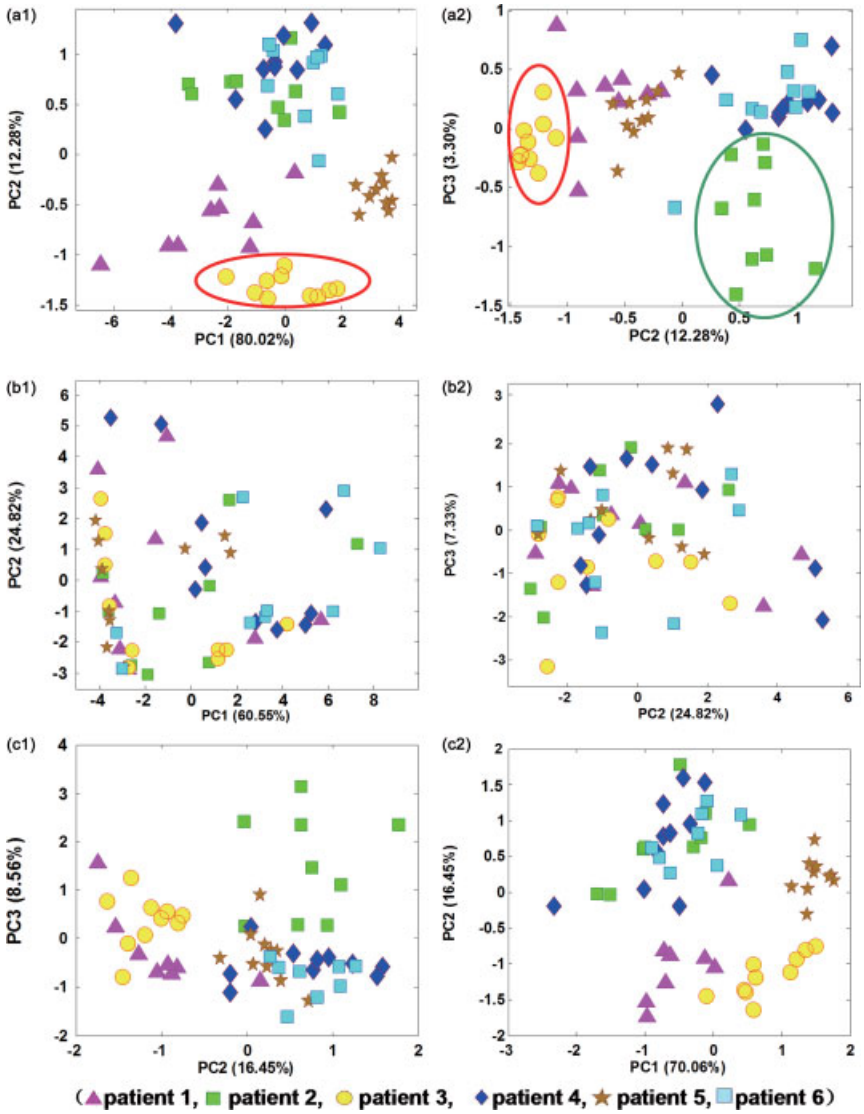

Figure 4. PCA score results for the differentiation of the human kidney stones. a1: Score plot of PC1 – PC2 based on positive SDAPCI; a2: score plot of PC2 – PC3 based on positive SDAPCI; b1: score plot of PC1 – PC2 based on negative SDAPCI; b2: score plot of PC2 – PC3 based on negative SDAPCI; c1: score plot of PC1 – PC2 based on the data without the highly abundant peaks; c2: score plot of PC2 – PC3 based on the data without the highly abundant peaks.

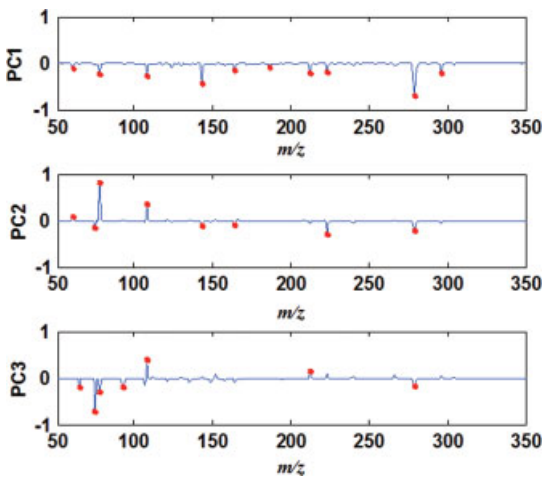

Figure 5. PCA loading results for the PCs based on positive SDAPCI.

scientific base for the differentiation of the melamine-induced kidney stones from the others and provides useful hints for further study on the formation mechanisms of melamine-induced kidney stones in the pathological research.

References

[1] F. Shirazi, F. Shahpourian, A. Khachian, F. Hosseini, A. H. Rad, S. Heidari, M. Sanjari. Personal characteristics and urinary stones. *Hong Kong J. Nephrol.* **2009**, *11*, 14.
[2] R. A. Anderson. A complementary approach to urolithiasis prevention. *World J. Urol.* **2002**, *20*, 294.
[3] C. W. Lam, L. Lan, X. Y. Che, S. Tam, S. S. Y. Wong, Y. Chen, J. Jin, S. H. Tao, X. M. Tang, K. Y. Yuen, P. K. H. Tam. Diagnosis and spectrum of melamine-related renal disease: plausible mechanism of stone formation in humans. *Clin. Chim. Acta* **2009**, *402*, 150.
[4] R. E. Baynes, G. Smith, S. E. Mason, E. Barrett, B. M. Barlow, J. E. Riviere. Pharmacokinetics of melamine in pigs following intravenous administration. *Food Chem. Toxicol.* **2008**, *46*, 1196.

[5] Z. C. Y. Chan, W. F. Lai. Revisiting the melamine contamination event in China: implications for ethics in food technology. *Trends Food Sci. Technol.* **2009**, *20*, 366.
[6] Y. C. Chiu, H. Y. Yang, S. H. Lu, H. K. Chiang. Micro-Raman spectroscopy identification of urinary stone composition from ureteroscopic lithotripsy urine powder. *J. Raman Spectrosc.* **2010**, *41*, 136.
[7] A. P. Evan, F. L. Coe, J. E. Lingeman, E. Worcester. Insights on the pathology of kidney stone formation. *Urol. Res.* **2005**, *33*, 383.
[8] I. H. Yarynovska, A. I. Bilyi. Optical spectroscopy of phosphatic urinary calculi – art. no. 66281c. In *Diagnostic Optical Spectroscopy in Biomedicine IV*, vol. 6628, **2007**, C6281.
[9] M. N. Ferrandino, S. A. Pierre, W. N. Simmons, E. K. Paulson, D. M. Albala, G. M. Preminger. Dual-energy computed tomography with advanced postimage acquisition data processing: improved determination of urinary stone composition. *J. Endourol.* **2010**, *24*, 347.
[10] Y. M. F. Marickar, P. Lekshmi, L. Varma, P. Koshy. Edax versus ftir in mixed stones. *Urol. Res.* **2009**, *37*, 271.
[11] L. Q. Jia, Y. Shen, X. M. Wang, L. J. He, Y. Xin, Y. X. Hu. Ultrasonographic diagnosis of urinary calculus caused by melamine in children. *Chin. Med. J.* **2009**, *122*, 252.
[12] N. Sun, Y. Shen, Q. Sun, X. R. Li, L. Q. Jia, G. J. Zhang, W. P. Zhang, Z. Chen, J. F. Fan, Y. P. Jiang, D. C. Feng, R. F. Zhang, X. Y. Zhu, H. Z. Xiao. Diagnosis and treatment of melamine-associated urinary calculus complicated with acute renal failure in infants and young children. *Chin. Med. J.* **2009**, *122*, 245.
[13] J. G. Wen, H. J. Yang, Y. Wang, G. X. Wang. The clinical analysis of urolithiasis in 165 infants and children with history of feeding melamine contaminated milk powder. *J. Urol.* **2009**, *181*, 1061.
[14] L. Zhang, L. L. Wu, Y. P. Wang, A. M. Liu, C. C. Zou, Z. Y. Zhao. Melamine-contaminated milk products induced urinary tract calculi in children. *World J. Pediatr.* **2009**, *5*, 31.
[15] R. G. Cooks, Z. Ouyang, Z. Takats, J. M. Wiseman. Ambient mass spectrometry. *Science* **2006**, *311*, 1566.
[16] H. W. Chen, B. Hu, X. Zhang. Principle and application of ambient mass spectrometry for direct analysis of complex samples. *Chin. J. Anal. Chem.* **2010**, *38*, 1069.
[17] Z. Takats, J. M. Wiseman, B. Gologan, R. G. Cooks. Mass spectrometry sampling under ambient conditions with desorption electrospray ionization. *Science* **2004**, *306*, 471.
[18] S. P. Yang, J. Han, Y. F. Huan, Y. J. Cui, X. Zhang, H. W. Chen, H. W. Gu. Desorption electrospray ionization tandem mass spectrometry for detection of 24 carcinogenic aromatic amines in textiles. *Anal. Chem.* **2009**, *81*, 6070.
[19] H. W. Chen, J. Meng, W. P. Wang, C. L. Chen, Z. C. Wang. Desorption electrospray ionization mass spectrometry for fast detection of alkaloids in fructus evodiae. *Chin. J. Anal. Chem.* **2009**, *37*, 237.
[20] I. Cotte-Rodriguez, Z. Takats, N. Talaty, H. W. Chen, R. G. Cooks. Desorption electrospray ionization of explosives on surfaces: sensitivity and selectivity enhancement by reactive desorption electrospray ionization. *Anal. Chem.* **2005**, *77*, 6755.
[21] R. B. Cody, J. A. Laramee, H. D. Durst. Versatile new ion source for the analysis of materials in open air under ambient conditions. *Anal. Chem.* **2005**, *77*, 2297.
[22] G. Morlock, Y. Ueda. New coupling of planar chromatography with direct analysis in real time mass spectrometry. *J. Chromatogr. A* **2007**, *1143*, 243.
[23] C. Petucci, J. Diffendal, D. Kaufman, B. Mekonnen, G. Terefenko, B. Musselman. Direct analysis in real time for reaction monitoring in drug discovery. *Anal. Chem.* **2007**, *79*, 5064.
[24] H. W. Chen, J. Zheng, X. Zhang, M. B. Luo, Z. C. Wang, X. L. Qiao. Surface desorption atmospheric pressure chemical ionization mass spectrometry for direct ambient sample analysis without toxic chemical contamination. *J. Mass Spectrom.* **2007**, *42*, 1045.
[25] S. P. Yang, J. H. Ding, J. Zheng, B. Hu, J. Q. Li, H. W. Chen, Z. Q. Zhou, X. L. Qiao. Detection of melamine in milk products by surface desorption atmospheric pressure chemical ionization mass spectrometry. *Anal. Chem.* **2009**, *81*, 2426.
[26] J. Wang, S. P. Yang, F. Y. Yan, Y. Liu, M. Li, Y. H. Song, Y. B. Zhan, H. W. Chen. Rapid determination of dimethoate in nanoliter of juice using surface desorption atmospheric pressure chemical ionization mass spectrometry. *Chin. J. Anal. Chem.* **2010**, *38*, 453.
[27] J. D. Harper, N. A. Charipar, C. C. Mulligan, X. R. Zhang, R. G. Cooks, Z. Ouyang. Low-temperature plasma probe for ambient desorption ionization. *Anal. Chem.* **2008**, *80*, 9097.
[28] N. Na, Y. Xia, Z. L. Zhu, X. R. Zhang, R. G. Cooks. Birch reduction of benzene in a low-temperature plasma. *Angew. Chem. Int. Ed.* **2009**, *48*, 2017.
[29] Y. Zhang, X. X. Ma, S. C. Zhang, C. D. Yang, Z. Ouyang, X. R. Zhang. Direct detection of explosives on solid surfaces by low temperature plasma desorption mass spectrometry. *Analyst* **2009**, *134*, 176.
[30] J. Shiea, M. Z. Huang, H. J. Hsu, C. Y. Lee, C. H. Yuan, I. Beech, J. Sunner. Electrospray-assisted laser desorption/ionization mass spectrometry for direct ambient analysis of solids. *Rapid Commun. Mass Spectrom.* **2005**, *19*, 3701.
[31] I. X. Peng, R. R. O. Loo, J. Shiea, J. A. Loo. Reactive-electrospray-assisted laser desorption/ionization for characterization of peptides and proteins. *Anal. Chem.* **2008**, *80*, 6995.
[32] I. X. Peng, J. Shiea, R. R. O. Loo, J. A. Loo. Electrospray-assisted laser desorption/ionization and tandem mass spectrometry of peptides and proteins. *Rapid Commun. Mass Spectrom.* **2007**, *21*, 2541.
[33] T. Harada, A. Yuba-Kubo, Y. Sugiura, N. Zaima, T. Hayasaka, N. Goto-Inoue, M. Wakui, M. Suematsu, K. Takeshita, K. Ogawa, Y. Yoshida, M. Setou. Visualization of volatile substances in different organelles with an atmospheric-pressure mass microscope. *Anal. Chem.* **2009**, *81*, 9153.
[34] S. P. Yang, H. W. Chen, Y. L. Yang, B. Hu, X. Zhang, Y. F. Zhou, L. L. Zang, H. W. Gu. Imaging melamine in egg samples by surface desorption atmospheric pressure chemical ionization tandem mass spectrometry. *Chin. J. Anal. Chem.* **2009**, *37*, 315.
[35] S. P. Yang, B. Hu, J. Q. Li, J. Han, X. Zhang, H. W. Chen, Q. Liu, Q. J. Liu, J. Zheng. Surface desorption atmospheric pressure chemical ionization mass spectrometry for direct detection melamine in powdered milk products. *Chin. J. Anal. Chem.* **2009**, *37*, 691.
[36] H. Xin, R. Stone. Tainted milk scandal Chinese probe unmasks high-tech adulteration with melamine. *Science* **2008**, *322*, 1310.
[37] R. N. S. Sodhi, H. W. Chen, S. P. Yang, B. Hu, X. Zeng, R.-H. Xiao. ToF-SIMS analysis of kidney stones possibly induced by the ingestion of melamine-containing milk products. *Surf. Interface Anal.* **2011**, *43*, 313.
[38] B. Hu, X. J. Peng, S. P. Yang, H. W. Gu, H. W. Chen, Y. F. Huan, T. T. Zhang, X. L. Qiao. Fast quantitative detection of cocaine in beverages using nanoextractive electrospray ionization tandem mass spectrometry. *J. Am. Soc. Mass Spectrom.* **2010**, *21*, 290.
[39] L. Zhu, G. Gamez, H. W. Chen, K. Chingin, R. Zenobi. Rapid detection of melamine in untreated milk and wheat gluten by ultrasound-assisted extractive electrospray ionization mass spectrometry (EESI-MS). *Chem. Commun.* **2009**, *45*, 559.
[40] I. A. Mokhless, M. A. Sakr, H. M. Abdeldaeim, M. M. Hashad. Radiolucent renal stones in children: combined use of shock wave lithotripsy and dissolution therapy. *Urology* **2009**, *73*, 772.
[41] X. H. Dai, X. Fang, C. M. Zhang, R. F. Xu, B. Xu. Determination of serum uric acid using high-performance liquid chromatography (HPLC)/isotope dilution mass spectrometry (ID-MS) as a candidate reference method. *J. Chromatogr. B* **2007**, *857*, 287.
[42] R. N. S. Sodhi. Time-of-flight secondary ion mass spectrometry (ToF-SIMS): versatility in chemical and imaging surface analysis. *Analyst* **2004**, *129*, 483.
[43] J. E. Jackson. Principal components and factor-analysis.1. Principal components. *J. Qual. Technol.* **1980**, *12*, 201.
[44] B. C. Moore. Principal component analysis in linear-systems – controllability, observability, and model-reduction. *IEEE T. Automat. Contr.* **1981**, *26*, 17.
[45] E. O. Kajander, N. Ciftcioglu. Nanobacteria: an alternative mechanism for pathogenic intra- and extracellular calcification and stone formation. *Proc. Natl. Acad. Sci. USA* **1998**, *95*, 8274.